Letter

Environment assisted superballistic scaling of conductance

Madhumita Saha,[1,2,*] Bijay Kumar Agarwalla,[1,†] Manas Kulkarni,[2,‡] and Archak Purkayastha[3,4,5,§]

[1]*Department of Physics, Indian Institute of Science Education and Research Pune, Dr. Homi Bhabha Road, Ward No. 8, NCL Colony, Pashan, Pune, Maharashtra 411008, India*

[2]*International Centre for Theoretical Sciences, Tata Institute of Fundamental Research, Bangalore 560089, India*

[3]*School of Physics, Trinity College Dublin, College Green, Dublin 2, Ireland*

[4]*Centre for complex quantum systems, Aarhus University, Nordre Ringgade 1, 8000 Aarhus C, Denmark*

[5]*Department of Physics, Indian Institute of Technology, Hyderabad 502284, India*

(Received 12 September 2022; revised 17 June 2023; accepted 13 October 2023; published 31 October 2023)

We find that, in the presence of weak incoherent effects from surrounding environments, the low-temperature conductance of nearest-neighbor tight-binding fermionic chains exhibits a counter-intuitive monotonic growth with system length when Fermi energy is near the band edges, indicating a superballistic scaling. This fascinating environment-assisted superballistic scaling of conductance occurs over a finite but extended regime of system lengths. This regime can be systematically expanded by decreasing the coupling to the surrounding environments and by reducing temperature. This behavior is robust against weak disorder and slight shifts from band edge, although the extent of the superballistic scaling regime is affected by them. We give precise predictions of how the superballistic scaling regime depends on coupling to surrounding environments, disorder strength, shifts from band edge, and temperature. There is no corresponding analog of this behavior in isolated systems. The superballistic scaling stems from an intricate interplay of incoherent effects from surrounding environments and exceptional points of the system's transfer matrix that occur at every band edge.

DOI: 10.1103/PhysRevB.108.L161115

Introduction. The resistance of a normal metal wire is proportional to its length, indicating diffusive transport. As a result, the metal's resistivity, given by resistance per unit length per unit cross-sectional area, is well defined. Deviation from this diffusive behavior, which leads to ill-defined resistivity, can be seen in a variety of situations, particularly in low-dimensional systems, and has been of great research interest [1–12]. Even outside of the diffusive regime, resistance generically increases with system length. The main exception is that of perfectly ballistic transport where resistance does not scale with system length [13–17].

In this letter, we demonstrate the possibility of behavior different from all of the above: resistance of a wire can decay monotonically over a finite but large regime of system lengths. In other words, there exists a regime in which conductance, i.e., the inverse of resistance, can increase monotonically with system length, thereby exhibiting superballistic scaling. This rather counter-intuitive behavior occurs close to zero temperature near the band edges of the system, assisted by weak incoherent effects from the surrounding environments. The regime exhibiting superballistic scaling systematically expands on weakening the system's coupling to its surrounding environments without completely isolating it from them.

We find this intriguing behavior by combining concepts from non-Hermitian physics [18–21] with those from quantum chemistry and mesoscopic physics. Borrowing from the latter, we model the surrounding environments by Büttiker voltage probes (BVPs) [22–37]. We show that the superballistic scaling of conductance near every band edge arises from an interplay of the incoherent effects from the BVPs and exceptional points (EPs) of the system's transfer matrix that occurs at every band edge [38]. The transfer matrix is a non-Hermitian matrix that appears in scattering theory. It plays a fundamental role in determining the band structure of the system and its transport properties [39–41]. To our knowledge, the role of non-Hermitian properties of the transfer matrix on environment-assisted transport has remained completely unexplored, despite the latter being investigated both theoretically and experimentally, across physics, chemistry, and biology [27–29,35,42–61].

It is worth mentioning that the term "superballistic" has been used in various separate contexts. In some experiments, conductance larger than the maximum conductance of free electrons has been termed superballistic [62–64]. In a separate set of works, faster-than-ballistic spread of an initially localized wavepacket has been explored both theoretically and experimentally [65–67]. However, to our knowledge, the superballistic scaling of conductance with system length has not been reported before. Unlike the spread of an initially localized wavepacket, this feature crucially requires presence of incoherent effects from surrounding environments and therefore cannot be seen in an isolated system.

Lattice chain with BVPs. We consider a nearest-neighbor tight-binding lattice chain consisting of N sites. For simplicity, we consider the single-band Hamiltonian given by $\hat{H}_C = \sum_{n=1}^{N-1} g(\hat{c}_n^\dagger \hat{c}_{n+1} + \hat{c}_{n+1}^\dagger \hat{c}_n) + \varepsilon \hat{H}_{\rm dis}$, where $\hat{c}_n$ is the

*madhumita.saha@acads.iiserpune.ac.in
†bijay@iiserpune.ac.in
‡manas.kulkarni@icts.res.in
§archak.p@phy.iith.ac.in

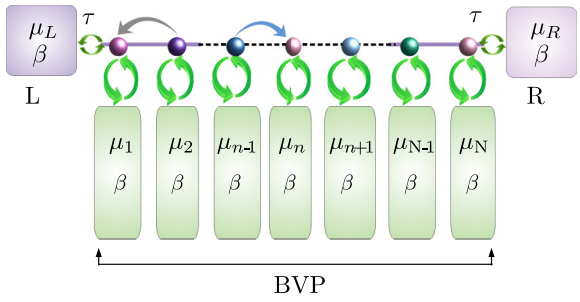

FIG. 1. A schematic of our setup showing a tight-binding chain subjected to left bath (L), right bath (R), and BVPs, all of which are at the same inverse temperature β. The left and right baths are coupled with strength τ, while the nth BVP is coupled with strength $\tau_P \nu^{(n)}$. The chemical potential of the probes $\mu_n, n = 1, 2, \cdots N$ are determined by demanding the zero-particle current between nth site and nth probe.

fermionic annihilation operator at the nth site. The Hamiltonian $\hat{H}_{\rm dis}$ contains random quadratic disorder terms in onsite energies and hopping. The parameter ε controls the overall strength of disorder. This chain is attached to a source bath with chemical potential μ_L at the left end, i.e, at first site, and a drain bath with chemical potential μ_R at the right end, i.e, at Nth site, which drives a current through the chain. Each bath is modeled via an infinite number of fermionic modes, and the system bath couplings are taken bilinear and number conserving. For simplicity, we consider the wide-band limit, with τ giving the effective strength of coupling with the left and right baths. The source and drain can be arbitrarily strongly coupled, we do not put any restriction on the magnitude of τ.

This lattice chain is subject to weak incoherent effects from surrounding environments apart from the source-drain baths. This is modeled by attaching BVPs at all the sites. These are baths similar to the source and drain baths, except that their chemical potentials $\{\mu_n\}$ are such that there is no average particle current into each of them. The temperature of all the baths are considered the same, given by inverse temperature β. The microscopic Hamiltonian $\hat{H}$ for this whole setup can be written as $\hat{H} = \hat{H}_C + \hat{H}_L + \hat{H}_R + \sum' \hat{H}_{P_n} + \hat{H}_{CL} + \hat{H}_{CR} + \sum' \hat{H}_{CP}^{(n)}$. $\hat{H}_L$ is the Hamiltonian of the left bath (source), $\hat{H}_R$ is the Hamiltonian of the right bath (drain), $\hat{H}_{P_n}$ is the Hamiltonian of the probe attached to the nth site of the system, $\hat{H}_{CL}$, $\hat{H}_{CR}$, and $\hat{H}_{CP}^{(n)}$ are the Hamiltonians which describe the coupling of central system with source, drain, and nth probe, respectively, and $\sum'$ denotes sum over the sites where the BVPs are attached. A schematic of our entire setup is shown in Fig. 1. We describe the setup in terms of the retarded nonequilibrium Green's function (NEGF) of the system, given by $G(\omega) = [\omega \mathbb{I} - H_C - \Sigma_L(\omega) - \Sigma_R(\omega) - \sum_{n=1}^{N} \Sigma_{P_n}(\omega)]^{-1}$. Here $\mathbb{I}$ is the $N \times N$ identity matrix, H_C is the $N \times N$ single particle Hamiltonian corresponding to $\hat{H}_C$, and $\Sigma_L(\omega)$, $\Sigma_R(\omega)$, $\Sigma_{P_n}(\omega)$ are the retarded self-energy matrices of the left, right, and probe baths, respectively, the only nonzero elements of which are $[\Sigma_L(\omega)]_{11} = -i\tau/2$, $[\Sigma_R(\omega)]_{NN} = -i\tau/2$, and $[\Sigma_{P_n}(\omega)]_{nn} = -i\tau_P \nu^{(n)}/2$. We will consider both the case of constant coupling to BVP, i.e, $\nu^{(n)} = 1$, and the case of disordered coupling to BVP, where $\nu^{(n)} > 0$, but otherwise random. Let us also define the average coupling to the probes $\overline{\tau}_P = \tau_P \overline{\nu}$, where $\overline{\nu}$ is the average value of $\nu^{(n)}$.

To describe conductance, we choose $\mu_R = \epsilon_F$, $\mu_L = \epsilon_F + \delta\mu$, $\mu_n = \epsilon_F + \delta\mu_n$, where ϵ_F is the Fermi energy. The conductance is then given by Landauer-Büttiker formula as [22–32,68]

$$\mathcal{G}(\epsilon_F) = \tau^2 |G_{1N}(\epsilon_F)|^2 + \tau^2 \tau_P \sum_{n,j=1}^{N} \nu^{(j)} |G_{Nn}(\epsilon_F)|^2 \mathcal{W}_{nj}^{-1}(\epsilon_F) |G_{j1}(\epsilon_F)|^2. \tag{1}$$

Here the elements of the $N \times N$ matrix $\mathcal{W}(\epsilon_F)$ are

$$\mathcal{W}_{nj} = -\tau_P \nu^{(j)} |G_{nj}|^2, \quad \forall\, n \neq j,$$
$$\mathcal{W}_{nn} = \tau(|G_{n1}|^2 + |G_{nN}|^2) + \tau_P \sum_{j \neq n}^{N} \nu^{(j)} |G_{nj}|^2, \tag{2}$$

where we have suppressed the argument ϵ_F for brevity. The above equations show that, knowing the retarded NEGF, the conductance in presence of the probes can be obtained. In absence of the probes [i.e., setting $\tau_P = 0$], the conductance is given by $\mathcal{G}^0(\epsilon_F) = \tau^2 |G^0_{1N}(\epsilon_F)|^2$, where $G^0(\epsilon_F)$ is the retarded NEGF in absence of the probes.

Main result. Let $\omega_b^{\pm}$ be the band edges of the system in the thermodynamic limit in absence of disorder. For our system $\omega_b^{\pm} = \pm 2g$. Then, our main result can be succinctly stated as follows:

$$\mathcal{G}(\omega_b^{\pm} \mp \eta) \text{ increases monotonically with N,}$$
$$\forall\ N_{\rm SB}^{(1)} < N < \min\left\{N_\eta, N_\varepsilon, N_\beta, N_{\rm SB}^{(2)}\right\}. \tag{3}$$

Here $N_{\rm SB}^{(1)} \sim \overline{\tau}_P^{-1/3}$, $N_{\rm SB}^{(2)} \sim \overline{\tau}_P^{-1/2}$ depend only on the average coupling to the probes, $N_\eta \sim \pi \eta^{-1/2}$ depends only on deviation from band edge, $N_\varepsilon \sim \sqrt{3}\pi \varepsilon^{-1/2}$ depends only on strength of disorder in the system, $N_\beta \sim \pi \beta^{1/2}$ depends only on temperature. Knowing these dependencies on various parameters, it is clear that this regime can be parametrically expanded by reducing $\overline{\tau}_P$, ε, η, and temperature. Thus, over a finite but extended regime of system lengths, there can be a superballistic scaling of conductance. Note that the possibility of such behavior, even in an idealized setting, was not known before. In the following, we show that this fascinating behavior is a consequence of EP of transfer matrix occurring at every band edge. We consider the upper band edge $\epsilon_F = \omega_b^+$. Due to particle-hole symmetry of the setup, exactly same results are obtained at the lower band edge $\epsilon_F = \omega_b^-$. Henceforth, we set the system hopping parameter to $g = 1$, which therefore sets our energy scale.

Without disorder, exactly at band edge, zero temperature: numerical results. First, we present numerical results in the complete absence of disorder, i.e., $\varepsilon = 0$, constant coupling to BVP, $\nu^{(n)} = 1$, take $\beta \to \infty$, and Fermi energy exactly at upper band edge $\epsilon_F = \omega_b^+$. In Fig. 2(a), we show plots of conductance with system length, for various small values of probe strength τ_P. For small N, we clearly see a remnant of the subdiffusive scaling $\mathcal{G}(\omega_b^+) \sim N^{-2}$ expected in absence of probes [38]. After this, we find the surprising superballistic regime $\mathcal{G}(\omega_b^+) \sim N^{\phi}$, $\phi > 0$ for a finite regime in system

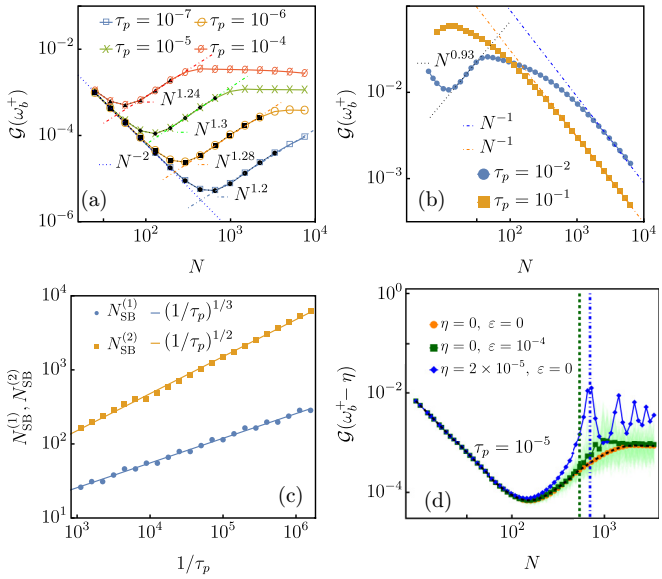

FIG. 2. (a) Behavior of $\mathcal{G}(\omega_b^+)$ with system length N for small values of τ_P, without any disorder. The black dots show approximate result obtained on replacing $G(\omega_b^+)$ by $G^0(\omega_b^+)$ (i.e., without the probes) in Eqs. (1) and (2). (b) Similar plots but at larger values of τ_P which captures the eventual crossover to conventional diffusive regime at large N. (c) The scaling of the start (end) of the superballistic regime $N_{\rm SB}^{(1)}$ ($N_{\rm SB}^{(2)}$) with τ_P^{-1}, the continuous line showing fit of $\tau_P^{-1/3}$ ($\tau_P^{-1/2}$). (d) The orange circles show $\mathcal{G}(\omega_b^+)$ with disordered but weak coupling to BVPs ($\tau_P = 10^{-5}$, $v^{(n)}$ randomly chosen between 0 and 1). The green squares show the same, with additional small disorder in the system ($\varepsilon = 10^{-4}$). The light green continuous lines show results for individual disorder realizations. The blue diamonds show conductance versus N, without any disorder in the system, but with slight shift in Fermi energy from band edge ($\eta = 2\times10^{-5}$). The black dotted plot shows $\mathcal{G}(\omega_b^+)$ without any disorder, but with $\tau_P \to \overline{\tau}_P = 0.5\tau_P$. The vertical green dashed line corresponds to $\sqrt{3}\pi\varepsilon^{-1/2}$ with $\varepsilon = 10^{-4}$. The vertical blue dot-dashed line corresponds to $\pi\eta^{-1/2}$, with $\eta = 2\times10^{-5}$.

length. The exponent ϕ is nonuniversal. Importantly, the superballistic regime expands as τ_P is reduced. Beyond the superballistic regime, the conductance starts saturating with system length, eventually decaying as we increase the system length further. Although not seen in our numerics for small τ_P up to the largest accessible N, we expect this slow decay with system length to eventually lead to standard diffusive behavior $\mathcal{G}(\omega_b^+) \sim N^{-1}$. This is captured for sufficiently large values of τ_P in Fig. 2(b).

To further analyze the superballistic regime, we extract from our numerics the onset and the termination of this regime. These correspond to the minimum and the following maximum of the plots in Fig. 2(a), respectively. In Fig. 2(c), we plot the starting (ending) system size of superballistic regime $N_{\rm SB}^{(1)}$ ($N_{\rm SB}^{(2)}$) as a function of τ_P^{-1}. We find that $N_{\rm SB}^{(1)} \sim \tau_P^{-1/3}$ and $N_{\rm SB}^{(2)} \sim \tau_P^{-1/2}$. For $\tau_P \ll 1$, we have $\tau_P^{-1/3} \ll \tau_P^{-1/2}$, which shows that the superballistic regime can be enhanced by reducing τ_P. Therefore, the extent of this superballistic regime $N_{\rm SB} = N_{\rm SB}^{(2)} - N_{\rm SB}^{(1)}$ increases as $N_{\rm SB} \sim \tau_P^{-1/2}$, with decrease in τ_P.

Origin of superballistic scaling: transfer matrix EPs. For nearest-neighbor one-dimensional systems, the retarded Green's function $G(\omega)$ is the inverse of a tridiagonal matrix. Using properties of tridiagonal matrices, in absence of any disorder, the elements of $G(\omega)$ can be written as [68] $G_{\ell j}(\omega) = (-1)^{\ell+j}\frac{\Delta_{1,\ell-1}(\omega)\Delta_{N-j,N}(\omega)}{\Delta_{1,N}(\omega)}$, where $\Delta_{1,\ell-1}(\omega)$, $\Delta_{N-j,N}(\omega)$, $\Delta_{1,N}(\omega)$ satisfy the following equations

$$\begin{pmatrix}\Delta_{1,N}(\omega)\\ \Delta_{1,N-1}(\omega)\end{pmatrix} = \begin{pmatrix}1 & \frac{i\tau}{2}\\ 0 & 1\end{pmatrix}[\mathbf{T}(\omega)]^N\begin{pmatrix}1\\ -\frac{i\tau}{2}\end{pmatrix},$$
$$\begin{pmatrix}\Delta_{1,\ell-1}(\omega)\\ \Delta_{1,\ell-2}(\omega)\end{pmatrix} = \begin{pmatrix}1 & \frac{i\tau}{2}\\ 0 & 1\end{pmatrix}[\mathbf{T}(\omega)]^{\ell-1}\begin{pmatrix}1\\ 0\end{pmatrix}, \quad (4)$$
$$\begin{pmatrix}\Delta_{N-j,N}(\omega)\\ \Delta_{N-j-1,N}(\omega)\end{pmatrix} = [\mathbf{T}(\omega)]^{N-j}\begin{pmatrix}1\\ -\frac{i\tau}{2}\end{pmatrix}. \quad (5)$$

In above, $\mathbf{T}(\omega)$ is a 2×2 matrix given by $\mathbf{T}(\omega) = \mathbf{T}^0(\omega) + \frac{i\tau_P}{4}(\mathbb{I}_2 + \sigma_z)$, where $\mathbf{T}^0(\omega) = \frac{\omega}{2}(\mathbb{I}_2 + \sigma_z) - i\sigma_y$ is the transfer matrix of the tight-binding chain, $\mathbb{I}_2$ is 2×2 identity matrix and $\sigma_{x,y,z}$ are the Pauli matrices. The above equations show that the nature of $\mathbf{T}(\omega)$ controls the system size scaling of various elements of the retarded NEGF in presence of BVPs, while $\mathbf{T}^0(\omega)$ does the same in their absence. It can be easily checked that $\mathbf{T}^0(\omega)$ has EPs at $\omega = \omega_b^{\pm}$. As has been recently shown [38], this behavior is a consequence of an antilinear symmetry of transfer matrices of nearest-neighbor tight-binding chains, which makes them pseudo-Hermitian. It holds in general even for multiband cases. As a consequence, in absence of the probes, conductance shows a universal subdiffusive scaling $\mathcal{G}^0(\omega_b^+) \sim N^{-2}$ at every band edge [38]. In our plots in Fig. 2, this is seen to survive up to a finite size $N_{\rm SB}^{(1)}$ for small τ_P.

For small τ_P and $N \ll N_{\rm SB}^{(2)}$ the leading order behavior should be captured by using $\mathbf{T}(\omega_b^+) \simeq \mathbf{T}^0(\omega_b^+)$. This is same as using Eqs.(1), (2), with $G(\epsilon_F)$ replaced by $G^0(\epsilon_F)$. This approximation can also be justified using a more careful, order-by-order perturbation in τ_P [68]. Conductance calculated in this approximation is shown by the black dots in Fig. 2(a). Indeed they overlap with the exact results in the entire subdiffusive and the superballistic regimes. This clearly establishes that the superballistic regimes stems from how the second term in Eq. (1), which embodies the effect of BVPs, is affected by the transfer matrix EP occurring at the band edge.

To explain the scaling of $N_{\rm SB}^{(1)}$ with τ_P, we look at the condition for observing the subdiffusive scaling. Clearly, this is seen in the regime where the effect of the probes is negligible. So, we calculate the expression for conductance up to the lowest order in τ_P. Since the second term in Eq. (1) is explicitly proportional to τ_P, in calculating all required matrix elements for that term, we simply set τ_P to zero. From Eq. (2), we see that this makes $\mathcal{W}(\epsilon_F)$ diagonal, which leads to $\mathcal{G} = \tau^2|G^0_{1N}|^2 + \tau\tau_P\sum_{\ell=1}^{N}\frac{|G^0_{\ell N}|^2|G^0_{1\ell}|^2}{|G^0_{1\ell}|^2+|G^0_{\ell N}|^2} + \mathcal{O}(\tau_P^2)$, where we have suppressed the argument ϵ_F for brevity. Due to transfer matrix EP at $\epsilon_F = \omega_b^+$, it can be checked that the second term in above expression diverges as N, while the first term decays as N^{-2} [68]. Clearly, $N_{\rm SB}^{(1)}$, which gives the end of the subdiffusive regime and the beginning of the superballistic regime, must correspond to the case where the two terms are

comparable $\tau {N_{\rm SB}^{(1)}}^{-2} \sim \tau_P N_{\rm SB}^{(1)}$. This directly gives $N_{\rm SB}^{(1)} \sim \tau_P^{-1/3}$, as has been numerically seen in Fig. 2(c). Thus, we conclude that the superballistic scaling comes from the second term in Eq. (1), in the regime where the EP of the transfer matrix governs its leading behavior.

To explain the scaling of $N_{\rm SB}^{(2)}$ with τ_P, we note that the presence of the probes makes $\mathbf{T}(\omega)$ always diagonalizable, with magnitude of one of the eigenvalues >1, as can be easily confirmed by direct calculation. Consequently, it can be shown that for $|\ell - j|$ large, $|G_{\ell j}(\omega)|^2 \sim e^{-|\ell-j|/\xi}$, with $\xi^{-1} = 2\kappa_1 = 2\log|\lambda_+|$ [68] where λ_+ is the eigenvalue of $\mathbf{T}(\omega)$ with higher magnitude. Whenever this is the case, the conductance in Eq. (1) gives diffusive scaling $\mathcal{G}(\omega) \sim N^{-1}$ for $N \gg \xi$, as has been shown in seminal work [32]. This holds for all values of ω. Hence, in presence of probes, at large enough system sizes, we always get diffusive behavior, as shown in Fig. 2(b). Thus, the superballistic scaling is observed for $N \lesssim \xi$. So, we have $N_{\rm SB}^{(2)} \sim \xi$. At band edges, to leading order on τ_P, the magnitude of eigenvalues of $\mathbf{T}(\omega)$ can be shown to be $|\lambda_\pm| \simeq 1 \pm \sqrt{\tau_P}$. This leads to $\xi^{-1} = 2\log|\lambda_+| \simeq 2\sqrt{\tau_P}$ [68], which then gives $N_{\rm SB}^{(2)} \sim \tau_P^{-1/2}$, as numerically seen in Fig. 2(c).

Effect of small disorder, small shifts from band edge, finite temperature. If disordered couplings to BVPs are considered, we numerically see that up to the superballistic regime, the conductance is almost exactly the same as the case of uniform coupling with the average strength, i.e., $\tau_P \to \overline{\tau}_P$. Figure 2(d) (orange circles) shows a representative plot, which completely overlaps with the corresponding uniform coupling result (black dotted line).

Disorder in the system onsite energies and hoppings, i.e, when $\varepsilon > 0$, nonperturbatively affects the single particle eigenstates and induces localization. But, for weak disorder, up to a finite system size, the eigenstates are affected only perturbatively, and the effects of localization do not manifest. It is within this regime that we expect the conductance scaling to also remain almost unaffected. Since we are considering the upper band edge, we look for the system size up to which perturbation theory holds for highest single-particle eigenstate. For the tight-binding chain, this system size can be calculated as $N_\varepsilon \sim \sqrt{3}\pi\varepsilon^{-1/2}$. Below N_ε we expect negligible effect of disorder. Figure 2(d) (compare green squares with black dotted line) shows a representative plot with numerical evidence of this.

The transfer matrix EPs are at the band edges of the system in the thermodynamic limit. At any finite system size N, let the maximum single-particle eigenvalue be ω_N^+. We have $\omega_b^+ - \omega_N^+ \simeq \pi^2 N^{-2}$ for the tight-binding chain. In absence of any BVPs, it can be checked that the subdiffusive scaling of conductance holds when $\omega_N^+ < \epsilon_F \leqslant \omega_b^+$. Since the superballistic regime occurs due to effect of the BVPs on the subdiffusive scaling regime, beyond this regime the superballistic scaling cannot be expected. For $\epsilon_F = \omega_b^+ - \eta$, with given η, this gives the length scale depending only on η, $N_\eta \sim \pi\eta^{-1/2}$, beyond which conductance should not be monotonically increasing. This behavior is shown in Fig. 2(d) (blue diamonds). We see that superballistic scaling function is drastically changed on shifting ϵ_F. However, note that even at $\epsilon_F = \omega_b^+$, the scaling function was not universal [see Fig. 2(a)].

Small finite temperature changes the expression for conductance [22–32], leading to an integration over energies around ϵ_F in a width $\sim 1/\beta$. So, by similar arguments as above, superballistic regime is expected to hold if temperature satisfies $\beta(\omega_b^+ - \omega_N^+) \simeq \beta\pi^2 N^{-2} \gg 1$. For a chosen β, this gives the system size $N_\beta \sim \pi\beta^{1/2}$ beyond which the superballistic regime is not expected. However, due to numerical instabilities, this regime is difficult to access computationally.

Combining all of the above, we arrive at our main result in Eq. (3). We reiterate that there is no assumption on strength of coupling to the source-drain leads τ, which need not be small. Below, we further generalize the result.

Generalization to multiband systems. Our analytical understanding shows that the superballistic regime stems from an interplay of the EPs of the transfer matrix, and the presence of BVPs. There is a transfer matrix EP at every band edge of any finite-ranged tight-binding chain, whether single-band or multiband [38]. Consequently, a superballistic regime will be seen near every band edge in all such cases. The multiband case can arise from presence of an additional periodic onsite potential in the system. Taking such a two-band case, the superballistic scaling can be easily explicitly confirmed [68].

Probes versus many-body interaction. Akin to BVPs, many-body interactions in the system can lead to inelastic scattering processes [23,48,69,70]. But, the superballistic scaling cannot be obtained with many-body interactions alone. This is because, at band edges, it can be argued that number-conserving many-body interactions have negligible effect due to vanishing particle or hole density [68]. Therefore, presence of surrounding environment is crucial for superballistic scaling. The simultaneous presence of BVPs and many-body interactions remains a challenging and interesting question beyond present analytical and numerical techniques.

Conclusions and outlook. We reveal how non-Hermitian properties of the transfer matrix affect environment-assisted transport, leading to superballistic scaling of conductance, a completely different regime of quantum transport. Physical effects of EPs of non-Hermitian matrices are of interest in the field of non-Hermitian physics and optics [18–21]. Different kinds of anomalous transport and their microscopic origins are of interest in statistical physics [8–12]. Environment-assisted transport is of interest in fields of mesoscopic physics [27–29,35–52], quantum many-body physics [53–56], quantum chemistry and biology [42–47], quantum thermodynamics [48,52], and also in quantum simulation experiments [57–61]. Our results therefore connect these different research directions. The practical implications of our results can be investigated in nanoscale quantum systems treated within density-functional theory [23,71–75], as well as in two-dimensional topological insulators [76,77] which provide effective one-dimensional ballistic transport channels.

Acknowledgments. M.S. acknowledges financial support through National Postdoctoral Fellowship (NPDF), SERB File No. PDF/2020/000992. B.K.A. acknowledges the

MATRICS Grant (Grant No. MTR/2020/000472) from SERB, Government of India, and the Shastri Indo-Canadian Institute for providing financial support for this research work in the form of a Shastri Institutional Collaborative Research Grant (SICRG). M.K. would like to acknowledge support from the Project No. 6004-1 of the Indo-French Centre for the Promotion of Advanced Research (IFCPAR), Ramanujan Fellowship (Grant No. SB/S2/RJN-114/2016), SERB Early Career Research Award (Grant No. ECR/2018/002085) and SERB Matrics Grant (Grant No. MTR/2019/001101) from the Science and Engineering Research Board (SERB), Department of Science and Technology, Government of India. M.K. acknowledges support of the Department of Atomic Energy, Government of India, under Project No. RTI4001. A.P. acknowledges funding from the European Union's Horizon 2020 Research and Innovation Program under the Marie Sklodowska-Curie Grant Agreement No. 890884. A.P. also acknowledges funding from the Danish National Research Foundation through the Center of Excellence "CCQ" (Grant Agreement No. DNRF156). This research was supported in part by the International Centre for Theoretical Sciences (ICTS) for participating in the program Physics with Trapped Atoms, Molecules and Ions (Grant No. ICTS/TAMIONs-2022/5). M.K. acknowledges support from the Infosys Foundation International Exchange Program at ICTS.

[1] X. Xu, L. F. C. Pereira, Y. Wang, J. Wu, K. Zhang, X. Zhao, S. Bae, C. Tinh Bui, R. Xie, J. T. L. Thong, B. H. Hong, K. P. Loh, D. Donadio, B. Li, and B. Özyilmaz, Nat. Commun. **5**, 3689 (2014).
[2] T. Meier, F. Menges, P. Nirmalraj, H. Hölscher, H. Riel, and B. Gotsmann, Phys. Rev. Lett. **113**, 060801 (2014).
[3] A. K. Majee and Z. Aksamija, Phys. Rev. B **93**, 235423 (2016).
[4] Q.-Y. Li, K. Takahashi, and X. Zhang, Phys. Rev. Lett. **119**, 179601 (2017).
[5] D. L. Nika, A. S. Askerov, and A. A. Balandin, Nano Lett. **12**, 3238 (2012).
[6] A. Purkayastha, A. Dhar, and M. Kulkarni, Phys. Rev. B **96**, 180204(R) (2017).
[7] A. Purkayastha, S. Sanyal, A. Dhar, and M. Kulkarni, Phys. Rev. B **97**, 174206 (2018).
[8] Z. Xu, Theor. Appl. Mech. Lett. **6**, 113 (2016).
[9] A. Dhar, A. Kundu, and A. Kundu, Front. Phys. **7**, 159 (2019).
[10] A. Dhar, Adv. Phys. **57**, 457 (2008).
[11] B. Bertini, F. Heidrich-Meisner, C. Karrasch, T. Prosen, R. Steinigeweg, and M. Žnidarič, Rev. Mod. Phys. **93**, 025003 (2021).
[12] G. T. Landi, D. Poletti, and G. Schaller, Rev. Mod. Phys. **94**, 045006 (2022).
[13] Y. Li, M. Amado, T. Hyart, G. P. Mazur, and J. W. A. Robinson, Commun. Phys. **3**, 224 (2020).
[14] J. Homoth, M. Wenderoth, T. Druga, L. Winking, R. G. Ulbrich, C. A. Bobisch, B. Weyers, A. Bannani, E. Zubkov, A. M. Bernhart, M. R. Kaspers, and R. Möller, Nano Lett. **9**, 1588 (2009).
[15] X. Liu, R. Stock, and W. Rudolph, Phys. Rev. B **72**, 195431 (2005).
[16] H. J. Li, W. G. Lu, J. J. Li, X. D. Bai, and C. Z. Gu, Phys. Rev. Lett. **95**, 086601 (2005).
[17] P. Debray, O. E. Raichev, P. Vasilopoulos, M. Rahman, R. Perrin, and W. C. Mitchell, Phys. Rev. B **61**, 10950 (2000).
[18] L. Feng, R. El-Ganainy, and L. Ge, Nat. Photonics **11**, 752 (2017).
[19] R. El-Ganainy, K. G. Makris, M. Khajavikhan, Z. H. Musslimani, S. Rotter, and D. N. Christodoulides, Nat. Phys. **14**, 11 (2018).
[20] R. El-Ganainy, M. Khajavikhan, D. N. Christodoulides, and S. K. Ozdemir, Commun. Phys. **2**, 37 (2019).
[21] Y. Ashida, Z. Gong, and M. Ueda, Adv. Phys. **69**, 249 (2020).
[22] M. Büttiker, Phys. Rev. Lett. **57**, 1761 (1986).
[23] J. Maassen, F. Zahid, and H. Guo, Phys. Rev. B **80**, 125423 (2009).
[24] C. J. Cattena, R. A. Bustos-Marún, and H. M. Pastawski, Phys. Rev. B **82**, 144201 (2010).
[25] D. Nozaki, C. Gomes da Rocha, H. M. Pastawski, and G. Cuniberti, Phys. Rev. B **85**, 155327 (2012).
[26] D. Nozaki, Y. Girard, and K. Yoshizawa, J. Phys. Chem. C **112**, 17408 (2008).
[27] M. Kilgour and D. Segal, J. Chem. Phys. **144**, 124107 (2016).
[28] M. Kilgour and D. Segal, J. Chem. Phys. **143**, 024111 (2015).
[29] R. Korol, M. Kilgour, and D. Segal, Comput. Phys. Commun. **224**, 396 (2018).
[30] M. Bandyopadhyay and D. Segal, Phys. Rev. E **84**, 011151 (2011).
[31] S. Bedkihal, M. Bandyopadhyay, and D. Segal, Eur. Phys. J. B **86**, 506 (2013).
[32] J. L. D'Amato and H. M. Pastawski, Phys. Rev. B **41**, 7411 (1990).
[33] D. Roy, J. Phys.: Condens. Matter **20**, 025206 (2008).
[34] D. Roy and A. Dhar, Phys. Rev. B **75**, 195110 (2007).
[35] E. Zerah-Harush and Y. Dubi, Phys. Rev. Res. **2**, 023294 (2020).
[36] M. Kulkarni, K. L. Tiwari, and D. Segal, New J. Phys. **15**, 013014 (2013).
[37] M. Kulkarni, K. L. Tiwari, and D. Segal, Phys. Rev. B **86**, 155424 (2012).
[38] M. Saha, B. K. Agarwalla, M. Kulkarni, and A. Purkayastha, Phys. Rev. Lett. **130**, 187101 (2023).
[39] Y. Last, Commun. Math. Phys. **151**, 183 (1993).
[40] L. Molinari, J. Phys. A: Math. Gen. **30**, 983 (1997).
[41] L. Molinari, J. Phys. A: Math. Gen. **31**, 8553 (1998).
[42] M. B. Plenio and S. F. Huelga, New J. Phys. **10**, 113019 (2008).
[43] P. Rebentrost, M. Mohseni, I. Kassal, S. Lloyd, and A. Aspuru-Guzik, New J. Phys. **11**, 033003 (2009).
[44] F. Caruso, A. W. Chin, A. Datta, S. F. Huelga, and M. B. Plenio, J. Chem. Phys. **131**, 105106 (2009).
[45] J. K. Sowa, J. A. Mol, G. A. D. Briggs, and E. M. Gauger, Phys. Chem. Chem. Phys. **19**, 29534 (2017).
[46] E. Zerah-Harush and Y. Dubi, J. Phys. Chem. Lett. **9**, 1689 (2018).
[47] R. Dutta and B. Bagchi, J. Phys. Chem. Lett. **8**, 5566 (2017).

[48] C. Chiaracane, A. Purkayastha, M. T. Mitchison, and J. Goold, Phys. Rev. B **105**, 134203 (2022).
[49] A. M. Lacerda, J. Goold, and G. T. Landi, Phys. Rev. B **104**, 174203 (2021).
[50] D. Dwiputra and F. P. Zen, Phys. Rev. A **104**, 022205 (2021).
[51] X. Turkeshi and M. Schiró, Phys. Rev. B **104**, 144301 (2021).
[52] M. Saha, B. P. Venkatesh, and B. K. Agarwalla, Phys. Rev. B **105**, 224204 (2022).
[53] M. V. Medvedyeva, T. c. v. Prosen, and M. Žnidarič, Phys. Rev. B **93**, 094205 (2016).
[54] M. Žnidarič, J. J. Mendoza-Arenas, S. R. Clark, and J. Goold, Annalen der Physik **529**, 1600298 (2017).
[55] M. Žnidarič, Phys. Rev. B **97**, 214202 (2018).
[56] J. J. Mendoza-Arenas, T. Grujic, D. Jaksch, and S. R. Clark, Phys. Rev. B **87**, 235130 (2013).
[57] C. Maier, T. Brydges, P. Jurcevic, N. Trautmann, C. Hempel, B. P. Lanyon, P. Hauke, R. Blatt, and C. F. Roos, Phys. Rev. Lett. **122**, 050501 (2019).
[58] R. D. J. León-Montiel, M. A. Quiroz-Juárez, R. Quintero-Torres, J. L. Domínguez-Juárez, H. M. Moya-Cessa, J. P. Torres, and J. L. Aragón, Sci. Rep. **5**, 17339 (2015).
[59] D. N. Biggerstaff, R. Heilmann, A. A. Zecevik, M. Gräfe, M. A. Broome, A. Fedrizzi, S. Nolte, A. Szameit, A. G. White, and I. Kassal, Nat. Commun. **7**, 11282 (2016).
[60] S. Viciani, M. Lima, M. Bellini, and F. Caruso, Phys. Rev. Lett. **115**, 083601 (2015).
[61] N. C. Harris, G. R. Steinbrecher, M. Prabhu, Y. Lahini, J. Mower, D. Bunandar, C. Chen, F. N. C. Wong, T. Baehr-Jones, M. Hochberg, S. Lloyd, and D. Englund, Nat. Photonics **11**, 447 (2017).
[62] R. Krishna Kumar, D. A. Bandurin, F. M. D. Pellegrino, Y. Cao, A. Principi, H. Guo, G. H. Auton, M. Ben Shalom, L. A. Ponomarenko, G. Falkovich, K. Watanabe, T. Taniguchi, I. V. Grigorieva, L. S. Levitov, M. Polini, and A. K. Geim, Nat. Phys. **13**, 1182 (2017).
[63] O. E. Raichev, Phys. Rev. B **106**, 085302 (2022).
[64] L. V. Ginzburg, C. Gold, M. P. Röösli, C. Reichl, M. Berl, W. Wegscheider, T. Ihn, and K. Ensslin, Phys. Rev. Res. **3**, 023033 (2021).
[65] A. Szameit, S. Stützer, T. Kottos, A. Tünnermann, S. Nolte, and D. N. Christodoulides, Superballistic transport and anomalous diffusion in inhomogeneous lattices, in *Frontiers in Optics 2012/Laser Science XXVIII*, OSA Technical Digest (online) (Optica Publishing Group, 2012), paper FTh2G.1. .
[66] S. Stützer, U. Naether, T. Kottos, R. A. Vicencio, M. I. Molina, A. Tünnermann, S. Nolte, D. N. Christodoulides, and A. Szameit, Observation of anomalous diffusion in a 1D optical random dimer, in *2013 Conference on Lasers & Electro-Optics Europe & International Quantum Electronics Conference CLEO EUROPE/IQEC* (IEEE, Piscataway, NJ, 2013), p. 1.
[67] S. Stützer, T. Kottos, A. Tünnermann, S. Nolte, D. N. Christodoulides, and A. Szameit, Observation of super-ballistic transport in hybrid ordered/disordered photonic lattices, in *Conference on Lasers and Electro-Optics 2012*, OSA Technical Digest (Optica Publishing Group, 2012), paper QF1H.6.
[68] See Supplemental Material at http://link.aps.org/supplemental/10.1103/PhysRevB.108.L161115 for additional analytical and numerical details.
[69] N. Sergueev, D. Roubtsov, and H. Guo, Phys. Rev. Lett. **95**, 146803 (2005).
[70] H. M. Pastawski, L. Foa Torres, and E. Medina, Chem. Phys. **281**, 257 (2002).
[71] M. Brandbyge, J.-L. Mozos, P. Ordejón, J. Taylor, and K. Stokbro, Phys. Rev. B **65**, 165401 (2002).
[72] A. Nitzan and M. A. Ratner, Science **300**, 1384 (2003).
[73] A. H. Larsen, J. J. Mortensen, J. Blomqvist, I. E. Castelli, R. Christensen, M. Dułak, J. Friis, M. N. Groves, B. Hammer, C. Hargus, E. D. Hermes, P. C. Jennings, P. B. Jensen, J. Kermode, J. R. Kitchin, E. L. Kolsbjerg, J. Kubal, K. Kaasbjerg, S. Lysgaard, J. B. Maronsson *et al.*, J. Phys.: Condens. Matter **29**, 273002 (2017).
[74] S. Kurth, D. Jacob, N. Sobrino, and G. Stefanucci, Phys. Rev. B **100**, 085114 (2019).
[75] S. Smidstrup, T. Markussen, P. Vancraeyveld, J. Wellendorff, J. Schneider, T. Gunst, B. Verstichel, D. Stradi, P. A. Khomyakov, U. G. Vej-Hansen, M.-E. Lee, S. T. Chill, F. Rasmussen, G. Penazzi, F. Corsetti, A. Ojanperä, K. Jensen, M. L. N. Palsgaard, U. Martinez, A. Blom *et al.*, J. Phys.: Condens. Matter **32**, 015901 (2020).
[76] L. Kou, Y. Ma, Z. Sun, T. Heine, and C. Chen, J. Phys. Chem. Lett. **8**, 1905 (2017).
[77] M. Z. Hasan and C. L. Kane, Rev. Mod. Phys. **82**, 3045 (2010).